

1 Article

# 2 Optimized Design of Modular Multilevel DC De-Icer 3 for High Voltage Transmission Lines

4 Jiazheng Lu, Qingjun Huang\*, Xinguo Mao, Yanjun Tan, Siguo Zhu and Yuan Zhu

5 State Key Laboratory of Disaster Prevention and Reduction for Power Grid Transmission and Distribution  
6 Equipment, State Grid Hunan Electric Company Limited Disaster Prevention and Reduction Center,  
7 Changsha, 410129, China;

8 Email: lujz1969@163.com (J.L.); dochuang@163.com (Q.H.); maoxg\_0@163.com; zhengyuan2017307@126.com (Y.T.);  
9 zhusiguo2005@163.com (S.Z.); zhuyuan1278@163.com (Y.Z.)

10 \* Correspondence: dochuang@163.com; Tel.: +86-0731-86332088

11

12

13 **Abstract:** Ice covering on overhead transmission lines would cause damage to transmission system  
14 and long-term power outage. Among various de-icing devices, modular multilevel converter  
15 (MMC) based DC de-icer (MMC-DDI) is recognized as a promising solution due to its excellent  
16 technical performance. Its principle feasibility has been well studied, but few literature discuss its  
17 economy or hardware optimization, thus the designed MMC-DDI for high voltage transmission  
18 lines is usually too large and too expensive for engineering applications. To fill this gap, this paper  
19 presents a quantitative analysis on the converter characteristics of MMC-DDI, and calculates the  
20 minimal converter rating and its influencing factors. It reals that, for a given de-icing requirement,  
21 the converter rating varies greatly with its AC-side voltage. Then an optimization configuration is  
22 proposed to reduce the converter rating and improve its economy. The proposed configuration is  
23 verified in a MMC-DDI for a 500kV transmission line as a case study. The result shows, in the case  
24 of outputting same de-icing characteristics, the optimized converter rating is reduced from 151  
25 MVA to 68 MVA, and total cost of MMC-DDI is reduced by 48%. This analysis and conclusion are  
26 conducive to the optimized design of multilevel DC de-icer, then to its engineering application.

27 **Keywords:** Converter, ice-melting, modular multilevel converter (MMC), optimization design,  
28 transmission line, static var generator (SVG)

29

## 30 1. Introduction

31 Ice covering on overhead transmission lines is a serious threat to the safe operation of power  
32 grids. Overweight ice would break wire or collapse the tower, and then cause disruption of power  
33 transmission and large-scale outage [1, 2]. The ice storms in North America 1998 [3], Germany 2005  
34 [4], and China 2008 [5] are good examples of such consequences. In order to protect the grid from  
35 ice disaster, dozens of anti-icing or de-icing methods have been proposed [1, 3, 5-7].

36 Among various de-icing methods, heating of ice-covered line conductors by electrical current is  
37 recognized as the most efficient engineering approach to minimize the catastrophic consequences of  
38 severe ice events [7-8]. Because it can eliminate the ice covered on hundreds of kilometers of line  
39 within an hour, meanwhile without damaging the grid structure or polluting the environment. Both  
40 AC and DC current can be used to melt ice, but the AC ice-melting is usually used for transmission  
41 lines up to 110kV, while the DC ice-melting is more recommended for higher voltage lines up to  
42 500kV transmission lines [3, 4]. In DC de-icing system, the most critical part is the DC de-icer (DDI)  
43 which generates the required ice-melting DC voltage and current.

44 Nowadays, the most widely adopted DDI is thyristor-based line-commutated converter (LCC),  
45 derived from the conventional HVDC technology. It has been widely used in Russia, Canada, China

46 [5, 9, 10]etc. Due to the inherent characteristics of thyristor, LCCs require multi-winding transformer,  
47 a series of harmonic filters and a large number of shunt capacitors to meet grid requirements. Thus,  
48 it occupies a large site area, and is bulky, inflexible, and costly. In order to overcome these  
49 shortcomings, many proposed to construct the DC de-icer using voltage source converter (VSC). In  
50 [11], a 3-level static synchronous compensator (STATCOM) was proposed for de-icer application. It  
51 can present excellent harmonic and reactive power features, but it requires complicated transformer  
52 and high-power 3-level converters up to 100MVA. Moreover, its output DC voltage has to exceed its  
53 AC-side voltage, namely, it has a limited DC voltage output range.

54 In the last few decades, the modular multilevel converter (MMC) topology has been rapidly  
55 developed and widely used in many high-voltage and medium-voltage applications [12, 13]. It can  
56 output a smooth and nearly ideal sinusoidal voltage with little filters, and it is modularity,  
57 scalability, facile, and flexible. In [14], a MMC-based DC de-icer (MMC-DDI) with full-bridge  
58 submodules (SM) was presented, and then it was further studied in [15-17]. It inherits all the  
59 aforesaid advantages of MMC topology. Moreover, it can provide both buck and boost functions for  
60 dc-link voltage, thus has a wide DC output voltage range to satisfy the de-icing requirements of  
61 different line lengths and different conductor sizes. In addition, it can be operated as a static var  
62 generator (SVG) to provide reactive power compensation for the grid. Due to these advantages, the  
63 MMC-DDI is recognized as a promising de-icing solution [15]. Since MMC-DDI was first proposed  
64 in 2013[14], its operation principle and control optimization have been further studied in [15-17].  
65 However, these literatures mainly focus on the technical feasibility of MMC-DDI, and pay little  
66 attention to its economy or hardware optimization. According to the existing MMC-DDI circuit  
67 configuration, some cases are designed for high voltage transmission lines up to 500kV. It is found  
68 that the MMC-DDI usually has far larger converter rating than its output ice-melting power,  
69 resulting in a poor economy to apply.

70 To address this issue, this paper presents a quantitative analysis on the converter characteristics  
71 of MMC-DDI, and then calculates the required converter rating and its influencing factors. It reveals  
72 that, for a certain DC de-icing requirement, converter rating varies greatly with its AC-side voltage,  
73 and then an optimized design method is proposed to improve the economy of MMC-DDI. Finally, a  
74 design example and its corresponding simulation results are given. As this case shown, under the  
75 same de-icing outputting characteristics, the optimized converter rating is reduced from 151MVA  
76 to 68MVA, and the total cost of MMC-DDI system is reduced by 48%.

## 77 2. Circuit configuration and operation principle

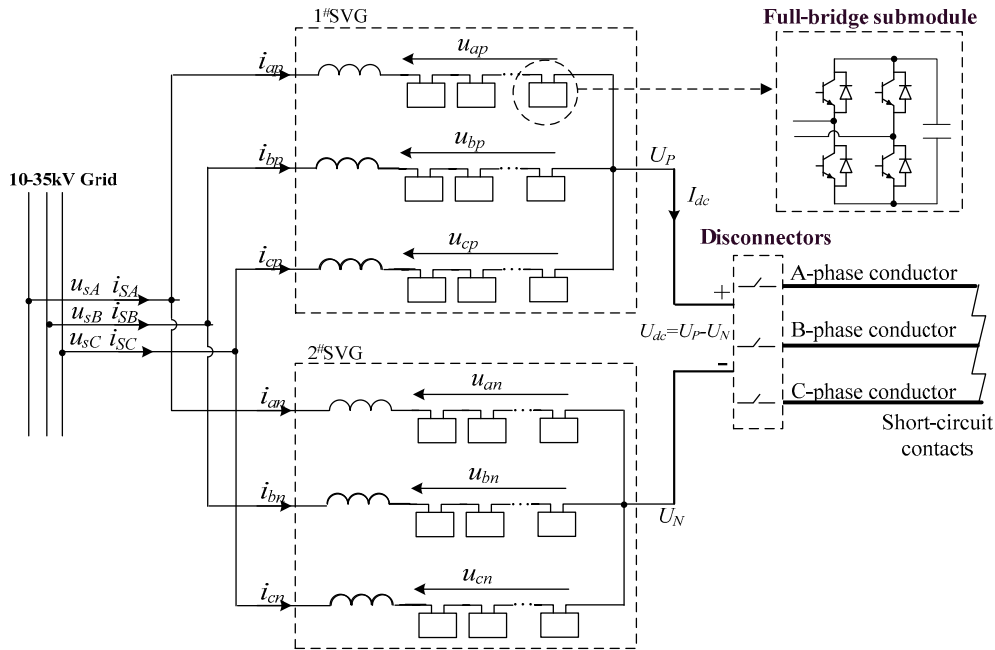
78 The circuit configuration of the MMC-DDI is shown in Figure 1[14-16]. It contains two sets of  
79 star-configured arms and each arm has several full-bridge SMs along with a connection reactance.  
80 Structurally speaking, it can be viewed as a pair of three-phase star-configured SVGs. The AC  
81 terminals of these two SVGs are in parallel and connected to the grid, whereas their neutral points  
82 are respectively led out as the DC positive and negative poles of MMC-DDI, and then connected to  
83 the ice-covered overhead lines through a set of de-icing disconnectors.

84 Since MMC-DDI can provide both buck and boost functions for dc-link voltage, it theoretically  
85 does not require a transformer to supply a wide and adjustable DC output voltage. In the existing  
86 literatures [14-16], the AC terminal of MMC-DDI is directly connected to the distribution network  
87 with no transformer. This is considered as a major advantage of the MMC-DDI scheme, because it  
88 can save the cost and floor area of a transformer, making the device small, light, and compact[15].

89 According to the grid requirements, MMC-DDI can have two different operation modes:

- 90 • Ice-melting Mode. When there is icing line to melt in winter, the disconnectors are closed to  
91 connect the MMC-DDI and the ice-covered transmission line together, and the other terminal  
92 of the transmission line is artificially three-phase short-circuit to form a DC current loop. Then,  
93 the MMC-DDI provides a controlled DC voltage to generate the required current through the  
94 ice-covered line. At that time, the operation mode of MMC-DDI is similar to the MMC rectifier  
95 station in the VSC-HVDC transmission system, except that the DC-side output voltage almost  
96 remains unchanged in the VSC-HVDC system while it may vary with the line parameters in

97 the MMC-DDI system. And the typical control methods for the common MMC system are also  
 98 applicable to MMC-DDI system, such as the capacitor voltage control, the active and reactive  
 99 current control, the capacitor voltage balancing control, circulating current control etc.



100

101

**Figure 1.** Circuit configuration of MMC based DC de-icer (MMC-DDI).

102

103

104

- SVG Mode. When there is no icing line, the de-icing disconnectors can be open circuit. Then the upper three arms and the lower three arms can operate as two parallel conventional SVGs, and provide reactive power compensation or alleviate other power quality problems.

105

### 3. Converter characteristic of MMC-DDI

106

#### 3.1. Arm voltage and current

107

According to Kirchhoff's law, the dynamic equations of MMC-DDI can be expressed as:

$$\begin{cases} u_{sA} = Ri_{a1} + L \frac{d}{dt} i_{a1} + u_{ap} + U_p \\ u_{sB} = Ri_{b1} + L \frac{d}{dt} i_{b1} + u_{bp} + U_p \\ u_{sC} = Ri_{c1} + L \frac{d}{dt} i_{c1} + u_{cp} + U_p \end{cases} \quad (1)$$

108

109

110

111

Where  $u_{sA}$ ,  $u_{sB}$ , and  $u_{sC}$  are the AC-side input phase voltage of the converter.  $u_{ap}$ ,  $u_{bp}$ , and  $u_{cp}$  are the output voltage of upper three arms.  $U_p$  is the electric potential of the neutral point of 1#SVG, relative to the grid neutral point.  $i_{a1}$ ,  $i_{b1}$ , and  $i_{c1}$  are arm currents in 1#SVG.  $R$  and  $L$  represent the equivalent resistance and inductance of the connection reactance in each arm.

$$\begin{cases} u_{sA} = Ri_{a2} + L \frac{d}{dt} i_{a2} + u_{an} + U_n \\ u_{sB} = Ri_{b2} + L \frac{d}{dt} i_{b2} + u_{bn} + U_n \\ u_{sC} = Ri_{c2} + L \frac{d}{dt} i_{c2} + u_{cn} + U_n \end{cases} \quad (2)$$

112 Where  $u_{an}$ ,  $u_{bn}$ , and  $u_{cn}$  are the output voltage of lower three arms.  $U_n$  is the electric potential of the  
113 neutral point of 2#SVG, relative to the grid neutral point.  $i_{a2}$ ,  $i_{b2}$ , and  $i_{c2}$  are the arm currents in 2#SVG.

$$\begin{cases} i_{sa} = i_{a1} + i_{a2} \\ i_{sb} = i_{b1} + i_{b2} \\ i_{sc} = i_{c1} + i_{c2} \end{cases} \quad (3)$$

114 Where  $i_{sA}$ ,  $i_{sB}$ , and  $i_{sC}$  are the AC-side input phase current of the converter.

$$\begin{cases} I_{dc} = i_{a1} + i_{b1} + i_{c1} = -(i_{a2} + i_{b2} + i_{c2}) \\ U_{dc} = U_p - U_n \end{cases} \quad (4)$$

115 Where  $U_{dc}$  and  $I_{dc}$  are the DC-side output voltage and current of the MMC-DDI.

116 Generally, the voltage and current of each arm in the MMC-DDI are symmetrical, and the  
117 circulation current among these arms can be effectively suppressed if proper appropriate control is  
118 adopted, moreover, the voltage drop across the connection reactance is far less than other items in  
119 the voltage equation (1) (2).As a result, the arm voltages and currents can be expressed as:

$$\begin{cases} u_{ap} = \sqrt{2}U_m \sin(\omega t) - 0.5U_{dc} \\ u_{bp} = \sqrt{2}U_m \sin(\omega t - 120^\circ) - 0.5U_{dc} \\ u_{cp} = \sqrt{2}U_m \sin(\omega t + 120^\circ) - 0.5U_{dc} \end{cases} \quad (5)$$

$$\begin{cases} u_{an} = \sqrt{2}U_m \sin(\omega t) + 0.5U_{dc} \\ u_{bn} = \sqrt{2}U_m \sin(\omega t - 120^\circ) + 0.5U_{dc} \\ u_{cn} = \sqrt{2}U_m \sin(\omega t + 120^\circ) + 0.5U_{dc} \end{cases} \quad (6)$$

$$\begin{cases} i_{ap} = \frac{\sqrt{2}}{2}I_m \sin(\omega t + \varphi) + \frac{I_{dc}}{3} \\ i_{bp} = \frac{\sqrt{2}}{2}I_m \sin(\omega t + \varphi - 120^\circ) + \frac{I_{dc}}{3} \\ i_{cp} = \frac{\sqrt{2}}{2}I_m \sin(\omega t + \varphi + 120^\circ) + \frac{I_{dc}}{3} \end{cases} \quad (7)$$

$$\begin{cases} i_{an} = \frac{\sqrt{2}}{2}I_m \sin(\omega t + \varphi) - \frac{I_{dc}}{3} \\ i_{bn} = \frac{\sqrt{2}}{2}I_m \sin(\omega t + \varphi - 120^\circ) - \frac{I_{dc}}{3} \\ i_{cn} = \frac{\sqrt{2}}{2}I_m \sin(\omega t + \varphi + 120^\circ) - \frac{I_{dc}}{3} \end{cases} \quad (8)$$

120 Where  $U_m$ ,  $I_m$  are the RMS values of the AC-side input phase voltage and current of MMC converter.

121 As shown in (5)-(8), the voltage/current of each arm contains both the AC and DC components.

122 Moreover, their peak values are the same for each arm, and can be expressed as

$$\begin{cases} I_{\text{arm\_peak}} = \frac{\sqrt{2}}{2}I_m + \frac{1}{3}I_{dc} \\ U_{\text{arm\_peak}} = \sqrt{2}U_m + 0.5U_{dc} \end{cases} \quad (9)$$

123 Where  $I_{arm\_peak}$ ,  $U_{arm\_peak}$  present the peak values of arm current and arm voltage.

124 According to (5)-(8), the RMS values of arm voltage and current can be expressed as

$$\begin{cases} I_{arm\_RMS} = \sqrt{\frac{1}{2}I_m^2 + \frac{1}{9}I_{dc}^2} \\ U_{arm\_RMS} = \sqrt{2U_m^2 + \frac{1}{4}U_{dc}^2} \end{cases} \quad (10)$$

125 Where  $I_{arm\_RMS}$ ,  $U_{arm\_RMS}$  present the RMS values of arm current and arm voltage.

126 Compared with that of the common SVG, the converter voltage/current in the MMC-DDI has  
127 different characteristics:

128 (1) The arm voltage/current of MMC-DDI contains both DC and AC components. While in the  
129 conventional SVG, there is only AC component.

130 (2) The arm voltage/current no more equals to the AC-side input voltage/current in MMC-DDI.

131 (3) The peak value of the arm voltage/current is no longer  $\sqrt{2}$  times of its RMS value.

132 Due to these differences, although the MMC-DDI is structurally similar to a pair of common  
133 star-connected SVGs, their inner converter characteristics are quite different.

### 134 3.2. Influence of AC side input voltage

135 Under normal operating condition, the AC side input active power of the MMC converter is  
136 substantially equal to its DC side output power (neglecting tiny converter loss). According to the  
137 power balance between the AC and DC sides, the output DC ice-melting power can be obtained:

$$P_{dc} = U_{dc} I_{dc} = 3I_m U_m \cos \varphi \quad (11)$$

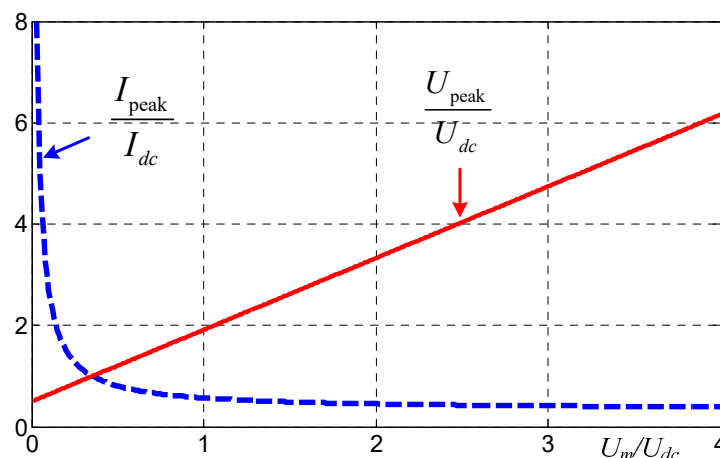
138 Where  $P_{dc}$  is the output ice-melting power,  $\cos \varphi$  is AC-side power factor and generally  $\cos \varphi = 1.0$ .

139 With (11), the AC-side input current of converter can be expressed as

$$I_m = \frac{U_{dc}}{3U_m \cos \varphi} I_{dc} \quad (12)$$

140 Substituting (12) into (9), the peak values of arm voltage and arm current can be expressed as

$$\begin{cases} I_{arm\_peak} = \left( \frac{\sqrt{2}}{6 \cos \varphi} \frac{U_{dc}}{U_m} + \frac{1}{3} \right) I_{dc} \\ U_{arm\_peak} = \left( \sqrt{2} \frac{U_m}{U_{dc}} + 0.5 \right) U_{dc} \end{cases} \quad (13)$$



141

142

**Figure 2.** Influence of AC side input voltage on arm current and arm voltage peaks

143 According to (13), the influence of AC side input voltage on the arm voltage and current peaks  
 144 can be plot and shown in Figure 2. As it shown, for a certain DC ice-melting requirement, with the  
 145 increasing of AC-side voltage , arm voltage peak increases linearly (but not proportionally) while  
 146 arm current peak decreases and tends to  $1/3 I_{dc}$ . This is quite different from common SVG. In a SVG,  
 147 in the case of a certain output reactive power, with the increasing of the AC-side voltage, the arm  
 148 voltage peak increases proportionally while the arm current peak decreases and tends to 0.

### 149 3.3. Converter Rating of MMC-DDI

150 In a power electronics system, the converter rating is an important technical indicator because  
 151 device cost is closely related with the converter rating. For a MMC converter, its converter rating is  
 152 mainly determined by the arm voltage peak and arm current peak, because they largely determines  
 153 the size and quantity of submodules, and then determines the main hardware of the converter.  
 154 Therefore, the converter rating of the MMC-based devices can be collectively defined as

$$S_c = \sum_1^n \frac{U_{pi} I_{pi}}{2} \quad (14)$$

155 Where  $S_c$  presents the converter rating,  $n$  presents the total number of arms.  $U_{pi}, I_{pi}$  are the output  
 156 voltage and current peak of the  $i$ -th arm.

157 For a conventional star-connected SVG, there are three arms, and the current peak of each arm  
 158 is approximately equal to the AC side phase current while arm voltage peak is approximately equal  
 159 to the AC-side phase voltage (ignoring the voltage drop across the connection reactance). Then its  
 160 converter rating can be expressed as

$$S_c = 3 \frac{U_p I_p}{2} = 3 \frac{\sqrt{2} U_{sp} \times \sqrt{2} I_{sp}}{2} = 3 U_{sp} I_{sp} = S_{out} \quad (15)$$

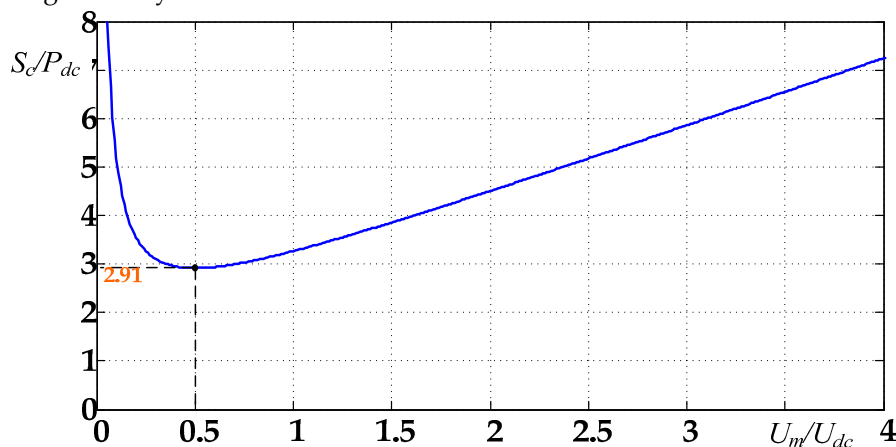
161 Where  $U_{sp}, I_{sp}$  are respectively the RMS values of AC-side phase voltage and phase current,  $S_{out}$   
 162 presents the output apparent power of SVG.

163 Indeed, equation (15) also applies to the delta-connected SVGs or a SVG group composed of  
 164 several converters. In summary, for any SVG, the converter rating can be directly characterized by  
 165 its rated output power.

166 For the MMC-DDI, the six arms share the same voltage and current peaks. Substituting (9) into  
 167 (16), and then the converter rating can be expressed as

$$S_c = 6 \frac{U_{arm\_peak} I_{arm\_peak}}{2} = 3 U_m I_m + \sqrt{2} U_m I_{dc} + \frac{3\sqrt{2}}{4} I_m U_{dc} + 0.5 U_{dc} I_{dc} \quad (16)$$

168 Compared with (15), there are 3 other items in (16), thus the converter rating characteristics of  
 169 MMC-DDI is significantly different from that of common SVG.



170  
171 **Figure 3.** Relationship of the converter rating of MMC-DDI with its AC-side voltage

172 Substituting (13) into (16) and considering  $\cos\varphi=1.0$ , the converter rating can be simplified as

$$S_c = 3 \left( \frac{\sqrt{2}}{6 \cos \varphi} \frac{U_{dc}}{U_m} + \frac{1}{3} \right) I_{dc} \cdot \left( \sqrt{2} \frac{U_m}{U_{dc}} + 0.5 \right) U_{dc} = \left( 1.5 + \frac{\sqrt{2}}{4} \frac{U_{dc}}{U_m} + \sqrt{2} \frac{U_m}{U_{dc}} \right) P_{dc} \quad (17)$$

173 With (17), the relationship of the converter rating of MMC-DDI with its AC-side voltage can be  
 174 calculated and shown as Figure 3. As it shown, under a certain DC-side output voltage and power  
 175 requirement, the converter rating varies greatly with its AC input voltage. It can be analytically  
 176 solved that when and only when  $U_m=0.5U_{dc}$ , the converter rating gets its minimum value, and the  
 177 minimum rating is 2.91 times of the output ice-melting power. This conclusion can be expressed as

$$S_{c\_min} = (1.5 + \sqrt{2}) P_{dc} \quad \text{when} \quad U_m = 0.5 U_{dc} \quad (18)$$

## 178 4. The proposed optimization design method

### 179 4.1 General design process of IMD

180 For any type of DC ice melting device, its design process generally follows these steps:

181 1) Step 1: According to the line parameters and meteorological conditions of the transmission  
 182 lines to be melted, calculate the required DC-side output de-icing current, voltage and power, and  
 183 then determine the rated DC-side output parameters of IMD.

184 For a given transmission line, its required de-icing current depends on many parameters, such  
 185 as conductor type, ambient temperature, wind velocity, ice thickness and de-icing duration etc. The  
 186 thermal behavior of overhead conductors has been well studied, and some formulas are given to  
 187 calculate the de-icing current in many industry standards, for example, the IEEE standard [18] and  
 188 CIGRE standard [19]. Generally, the de-icing current should be greater than the minimum de-icing  
 189 current and no more than the maximum endure current of line conductor. For some typical  
 190 conductor types used in China, the minimum de-icing current and the maximum endure current  
 191 are shown as Table A1[5]. In actual ice melting system, it generally tries to choose the intermediate  
 192 value of the maximum and minimum values as the rated de-icing current.

193 After determining the de-icing current, the required de-icing DC voltage can be calculated as

$$U_{dc} = k_{icing} R_{line} I_{icing} \quad (19)$$

194 Where  $I_{icing}$  is the required de-icing current,  $R_{line}$  is the phase resistance of transmission line.  $k_{icing}$   
 195 corresponds to the ice-melting mode,  $k_{icing}=2$  when the de-icing current is passed down one-phase  
 196 conductor and back along another, and  $k_{icing}=1.5$  when down one and back along the other two[16].

197 When there are several lines to be melted, the de-icing DC current and voltage of each line can  
 198 be calculated one by one, then the rated DC-side output parameters of the IMD is determined by  
 199 the output DC voltage range, the maximum de-icing current, and the maximum de-icing power.

200 2) Step 2: According to the optional voltage levels of the power substation as well as the rated  
 201 IMD output power, select the proper access voltage of the IMD.

202 For typical transmission lines, their DC ice-melting power is generally among several MW and  
 203 hundreds of MW. Within this range, the IMD is usually connected to the low-voltage distribution  
 204 network of the substation, generally 10kV or 35kV in China.

205 3) Step 3: According to the DC-side output parameter requirements and the grid access voltage,  
 206 design the internal structure and parameters of the IMD.

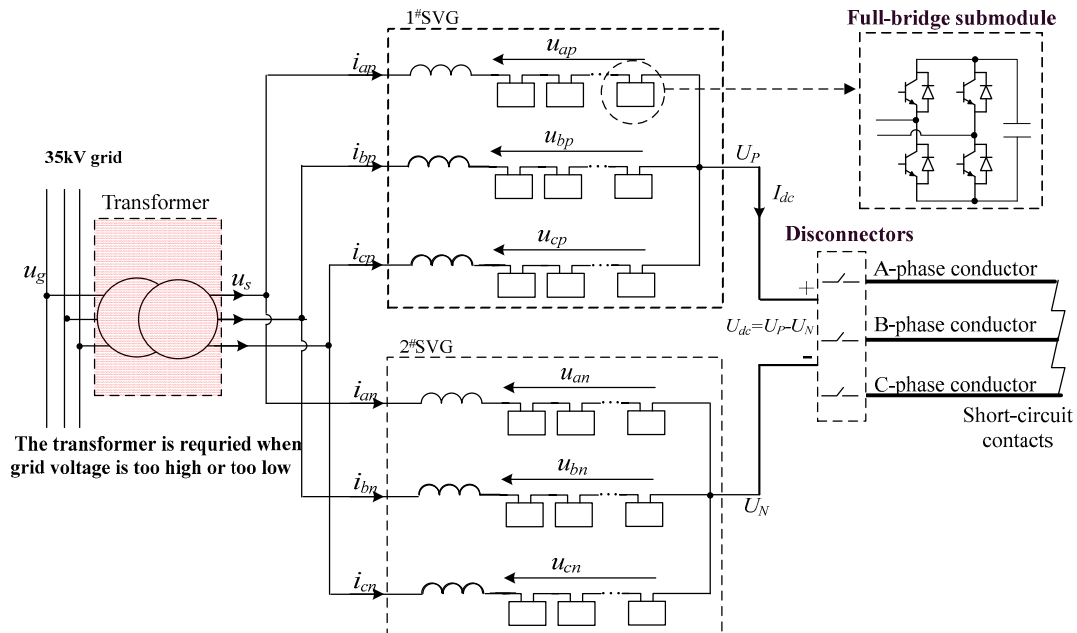
207 In the process of designing the internal IMD parameters, it is usually necessary to consider  
 208 both the technical feasibility and the economy.

### 209 4.2 The proposed circuit configuration and its economic analysis

210 According to the above calculation, for a certain ice-melting requirement, the converter rating  
 211 of MMC-DDI varies greatly with its AC-side voltage. Traditionally, MMC-DDI is directly connected

212 to the grid[14, 15], thus its AC-side input voltage always equals to the grid voltage. This may  
 213 correspond to very high converter rating, resulting in a poor economy. To solve such problem, this  
 214 paper proposes an optimization MMC-DDI configuration structure as shown in Figure 4, i.e., a  
 215 transformer should be inserted between the grid and the converter in some cases. In order to realize  
 216 this idea, there are two main questions:

- 217 A) When the transformer should be desired and when it is undesired?  
 218 B) If a transformer is inserted, what are the specifications and parameters of the transformer?



219  
 220

**Figure 4.** The proposed configuration structure of MMC-DDI

221 According to (11), when the power factor is controlled as  $\cos\varphi=1$ , the input apparent power of  
 222 MMC-DDI always equals to its DC side output power regardless of the AC-side voltage. Therefore,  
 223 if a transformer is inserted, the transformer rating only needs to equal to the output de-icing power  
 224 rather than the converter rating. In order to get the minimum converter rating as shown in (18), the  
 225 output phase voltage of the transformer can be set as  $U_m=0.5U_{dc}$ , corresponding to a line voltage  
 226  $\sqrt{3}\times 0.5U_{dc}$ . In summary, the specification of the transformer can be determined as

$$\begin{cases} S_{Tran} = P_{dc} \\ T_r = U_g / (\sqrt{3}\times 0.5U_{dc}) \end{cases} \quad (20)$$

227 Where  $S_{Tran}$  is the transformer rating,  $T_r$  is the transformer rating voltage ratio.

228 For the time of transformer insertion question, the cost of converter and transformer should be  
 229 compared. Since the MMC-DDI is rarely applied, it is difficult to obtain its market cost; here its cost  
 230 is estimated by referring to that of SVGs. That is due to two reasons, 1) MMC-DDI is structurally  
 231 equivalent to a pair of three-phase star-connected SVGs, 2) SVG has been widely used and its cost is  
 232 transparent. Table A2 shows the deal prices of several typical SVGs in China from 2013 to 2018.

233 As(15) shown, the converter rating of a SVG is approximately equal to its rated output power,  
 234 the converter cost can be directly evaluated with the SVG cost list in Table A2. As Table A2 shown,  
 235 SVG cost is basically proportional to the rating, and the unit cost is around 15,000 \$/Mvar. For some  
 236 SVGs over 60Mvar, the unit cost is slightly higher. This is because there are only a few applications  
 237 for such high-power SVGs, thus the R&D cost is high. On the other hand, high-power SVG usually  
 238 requires higher reliability and larger configuration margin, and this also increases the device cost.

239 When a transformer is inserted as Figure 4, the transformer would bring a cost itself. Table A3  
 240 shows the deal prices of several 10MVA-class rectifier transformers in China.

241 It can be seen that the cost of a 10 MVA rectifier transformer is about 86000 \$, about 1/2 of the  
 242 same rating SVG. Moreover, with the growth of transformer rating, the unit cost decreases rapidly.



243 For a 56 MVA transformer, its unit cost is 4400 \$/Mvar and about 1/3 of a similar rating SVG. For a  
244 100 MVA transformer, its unit cost reduces to 3300 \$/Mvar and about 1/6 of the same rating SVG.

245 In order to quantitatively compare the economics of the proposed configuration structure, the  
246 costs of the MMC-DDI with and without the transformer can be expressed as

$$\begin{cases} P_{no} = P_{con}(u_s = u_g) \\ P_{with} = P_{trans} + P_{con}(u_s = \sqrt{3} \times 0.5U_{dc}) \end{cases} \quad (21)$$

247 Where  $P_{no}$  presents the cost of MMC-DDI with no transformer,  $P_{con}(u_s = u_g)$  presents the cost of the  
248 MMC converter when its AC-side voltage equals to the grid voltage.  $P_{with}$  presents the cost of the  
249 MMC-DDI with a transformer;  $P_{trans}$  presents the transformer cost.  $P_{con}(u_s = \sqrt{3} \times 0.5U_{dc})$  presents the  
250 cost of the MMC converter with a AC-side input voltage of  $u_s = \sqrt{3} \times 0.5U_{dc}$ .

251 After inserting the transformer, the cost reduction of the total MMC-DDI can be expressed as:

$$\Delta P = P_{no} - P_{with} = \underbrace{P_{con}(u_s = u_g) - P_{con}(u_s = \sqrt{3} \times 0.5U_{dc})}_{\Delta P_{con}} - P_{trans} \quad (22)$$

252 Where  $\Delta P_{con}$  presents the cost saving of the converter.

253 As long as the cost reduction is greater than zero, namely, the converter cost saving is greater  
254 than the transformer cost, the proposed configuration structure is cost-effective. In order to obtain a  
255 quantitative guidance, here makes an approximation of the cost of converter and SVG.

256 1) The converter cost is approximately considered to be proportional to the converter rating.

257 2) The transformer cost is a quarter of the same rating MMC converter cost.

258 Based on the above approximation and considering (17), the equation (22) can be rewritten as

$$\Delta P = k_1 \left( 1.5 + \frac{\sqrt{6}}{4} \frac{U_{dc}}{U_g} + \sqrt{\frac{2}{3}} \frac{U_g}{U_{dc}} \right) P_{dc} - k_1 \times 2.91 P_{dc} - \frac{k_1}{2.5} P_{dc} = k_1 P_{dc} \left( \frac{\sqrt{6}}{4} \frac{U_{dc}}{U_g} + \sqrt{\frac{2}{3}} \frac{U_g}{U_{dc}} - 1.81 \right) \quad (23)$$

261 Where  $k_1$  presents the unit cost of MMC converter, it approximately equals to 15000\$ / Mvar.

262 With (23), it can be analytically solved that when  $U_g > 1.96U_{dc}$  or  $U_g < 0.25U_{dc}$ , the cost reduction is  
263 positive, namely, the insertion of the transformer is cost-effective.

### 264 4.3 Applicable scope of the proposed configuration

265 Compared with the traditional MMC-DDI structure, the proposed MMC-DDI configuration  
266 structure requires an extra transformer. It seems that this would increase the cost of the total system,  
267 and partially offset the advantages of the MMC topology. However, in fact, the converter rating of  
268 traditional MMC-DDI varies greatly with its AC-side voltage, thus the insertion of transformer can  
269 sometimes reduce the converter rating and its cost. As long as the reduction of the converter cost is  
270 sufficient to offset the transformer cost, the proposed MMC-DDI structure is cost-effective.

271 According to the cost comparison data of the converter and transformer in the previous section,  
272 the unit cost of a MMC converter is generally much higher than that of a conventional transformer,  
273 especially for large-capacity converters above 50MVA. Moreover, the saved converter rating by the  
274 introduction of a transformer is sometimes much higher than the transformer rating. Therefore, the  
275 introduction of the transformer is worthwhile in some cases. Under the cost model established in  
276 the previous section, it can be obtained that:

277 1) When the ratio of the grid line voltage to DC-side output voltage exceeds 1.96 or falls below  
278 0.25, the overall cost of MMC-DDI with the transformer is less than that with no transformer, i.e., a  
279 transformer can be inserted on the AC side of converter to improve the system economy.

280 2) When the ratio of the grid line voltage to the DC-side output voltage is among 0.25-1.96, the  
281 cost of the transformer exceeds the revenue that it brings. In that case, no transformer is required.

282 Indeed, for the common high-voltage transmission lines up to 500 kV, the required ice-melting  
 283 DC voltage is generally less than 15kV. Under such ice-melting voltage range, if the MMC-DDI is  
 284 connected to the 35kV distribution network, the grid voltage is more than 2 times of the ice-melting  
 285 DC voltage. In that case, the proposed MMC-DDI configuration as Figure 4 is more applicable than  
 286 the traditional MMC-DDI configuration as Figure 1. But if the MMC-DDI is connected to the 10kV  
 287 distribution network, the grid voltage is usually among 0.25-1.96 times of the DC-side voltage. In  
 288 that case, the traditional MMC-DDI configuration is more applicable.

## 289 5. Design Example and Simulation Result

### 290 5.1. A typical design example

291 In order to verify the above analysis and the proposed configuration, a design example of  
 292 MMC-DDI is given here. For a 500kV transmission line, the wire type is 4×LGJ-400, the line length is  
 293 40km, and its single-phase resistance is 0.72 Ω. The minimum ambient temperature along the line is  
 294 -5°C, and the maximum wind speed in winter is about 5m/s. In the 500kV substation at one end of  
 295 the transmission line, the distribution grid voltage is 35kV, corresponding a 20.2kV phase voltage.

296 With the data shown in Table A1, the required de-icing current of the above transmission line  
 297 should be between 3475-4768A. Within this range, the smaller the current, the longer the de-icing  
 298 process lasts. Considering a balance between ice-melting rapidity and IMD economics, the rated DC  
 299 de-icing current can be set as 4.0kA. Then with (19), the required de-icing voltage can be calculated  
 300 as 5.76kV( $2 \times 4.0\text{kA} \times 0.72 \Omega$ ). Thus, the rated de-icing output power is 23.2MW( $=5.76\text{kV} \times 4.0\text{kA}$ ).

301 If the MMC-DDI is directly connected into the 35kV grid without a transformer as [15], the  
 302 AC-DC voltage ratio  $U_m/U_{dc}$  is 3.5 (20.2kV/5.8 kV). According to (17) or Figure 3, the converter rating  
 303 will be 6.5 times of its output ice-melting power, i.e., it will reach up to 151MVA( $=6.5 \times 23.2\text{MW}$ ).  
 304 Such huge converter leads to high cost and poor economy.

305 With the formulas in chapter 3, the detailed electrical parameters of above MMC-DDI can be  
 306 calculated and then listed in Table 1. The voltage and current peaks of the six arms are respectively  
 307 31.5kV and 1.6kV, thus the converter is equivalent to two conventional star-connected SVGs and  
 308 each SVG has a 38.5kV rated line voltage ( $31.5\text{kV} / \sqrt{2} \times \sqrt{3}$ ), a 1.13kA rated current ( $1.6\text{kA} / \sqrt{2}$ ), a  
 309 75.4Mvar rating ( $\sqrt{3} \times 38.5\text{kV} \times 1.13\text{kA}$ ). Referring to the SVG price list in Table A2, the unit cost of  
 310 MMC converter can be approximated as 15000 \$/Mvar, and then the converter cost can be estimated  
 311 as about 2.26 million dollar ( $15000\$/\text{Mvar} \times 75.4 \times 2 = 2.26$  million). With respect to its 23.2MW  
 312 output de-icing power, such cost is too high to be acceptable.

313 **Table 1.** Electrical parameter comparison of the MMC-DDI under conventional configuration and  
 314 optimized configuration

Parameter	Symbol	Conventional configuration (With no transformer)	Optimized configuration (With transformer)
Rated DC voltage	$U_{dc}$	5.8kV	5.8kV
Rated DC current	$I_{dc}$	4.0kA	4.0kA
Rated output DC power	$P_{dc}$	23.2MW	23.2MW
AC-side phase voltage	$U_m$	20.2kV	2.9kV
AC-side phase current	$I_m$	0.38A	4.6kA
Arm voltage peak	$U_{arm\_peak}$	31.5kV	7.0kV
Arm current peak	$I_{arm\_peak}$	1.6kA	3.2kA
Converter rating	$S_c$	151MVA	68MVA
Transformer	-	None	23 MVA-35 kV/5 kV

315 If the proposed optimization method is adopted, a 23 MVA-35 kV/5 kV transformer should be  
 316 inserted between the MMC converter and the 35kV grid. At this time, the optimized MMC-DDI is

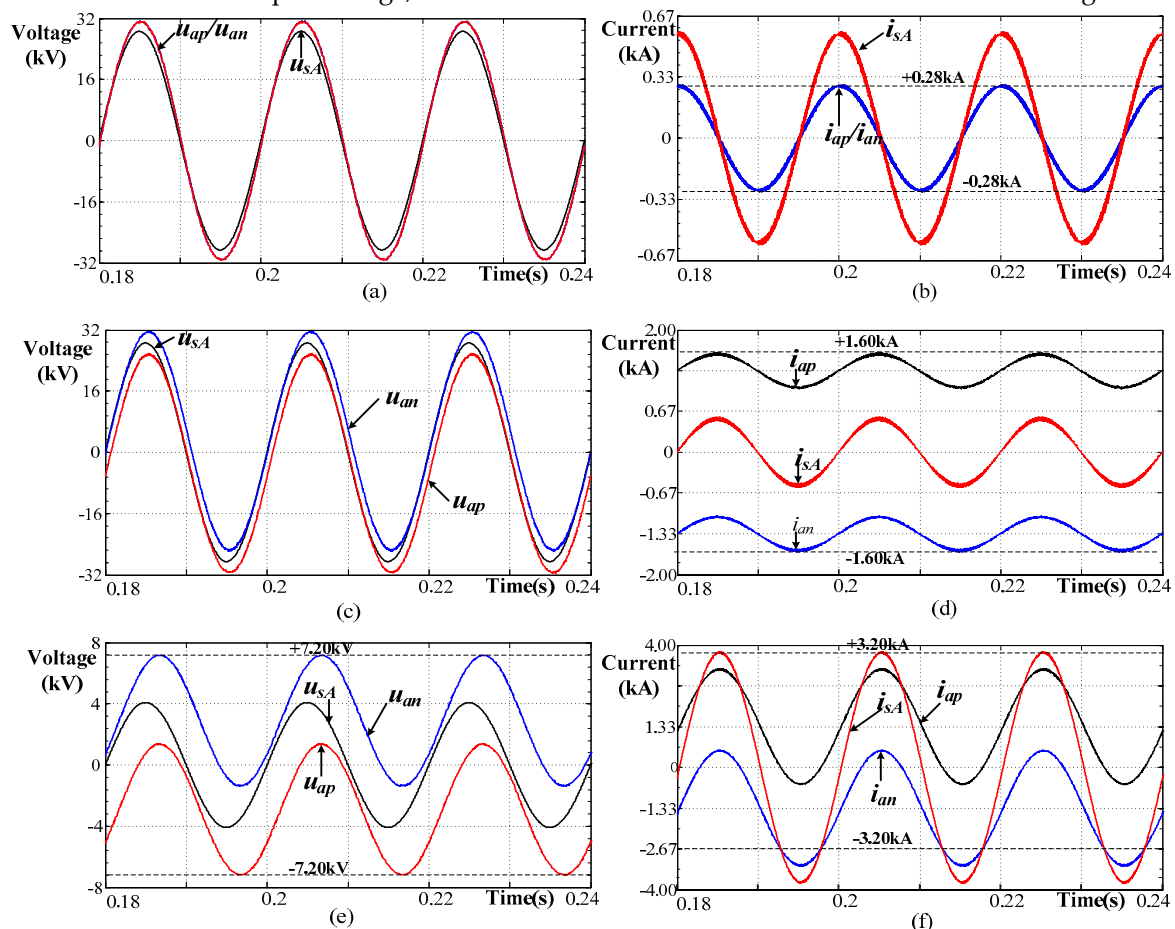
317 mainly composed of a MMC converter and a transformer, and the detailed electrical parameters of  
 318 MMC-DDI are also listed in Table 1. As it shown, the voltage and current peaks of the six arms are  
 319 7.0 kV and 3.2kV, thus the converter is equivalent to two common SVGs and each SVG has a rated  
 320 line voltage 8.57 kV ( $7.0\text{kV} / \sqrt{2} \times \sqrt{3}$ ), 2.26kA rated current ( $3.2\text{kA} / \sqrt{2}$ ) and 33.5 Mvar rating  
 321 ( $\sqrt{3} \times 8.57\text{kV} \times 2.26\text{kA}$ ). Considering the approximate SVG unit cost (15000 \$/ Mvar), the converter  
 322 cost can be estimated as 1.01 million dollar ( $15000 \text{ \$/Mvar} \times 33.5 \text{ Mvar} \times 2$ ). In addition, in Table A3,  
 323 the cost of a 24MVA transformer is 166000 \$. Then the total cost of the optimized MMC-DDI can be  
 324 estimated as 1.18 million dollar. The above cost comparison results are listed in Table 2. Compared  
 325 with the cost of the original MMC-DDI with no transformer, the optimized cost of the IMD device  
 326 has dropped by 48%.

327 **Table 2.** Cost comparison of the MMC-DDI under conventional configuration and optimized configuration

Component	Original cost (million dollar)	Optimized cost (million dollar)
Converter	2.26	1.01
Transformer	-	0.17
Total	2.26	1.18

## 328 5.2. Simulation Results

329 To verify the above analysis and calculation on the converter characteristic, a corresponding  
 330 MMC-DDI system is built in Matlab/Simulink, and the simulation parameters are set as given in the  
 331 previous section. For comparison, a dual-SVGs system ( $2 \times 11.6\text{Mvar}$ ), which is similar to Figure 1  
 332 but has no DC-side output voltage, is also simulated. The simulation results are shown in Figure 5.



333  
 334  
 335

Figure 5. Simulation results of the converter voltage and current. (a) arm voltage of the dual-SVGs system, (b) arm current of the dual-SVGs system, (c) arm voltage of the original MMC-DDI as Figure

336 1, (d) arm current of the original MMC-DDI as Figure 1, (e) arm voltage of the optimized MMC-DDI  
337 as Figure 4, (f) arm current of the optimized MMC-DDI as Figure 4

338 As Figure 5a and 5b shown, in the dual-SVGs system, the arm voltage is slightly higher than the  
339 AC-side phase voltage, and the arm current equals to half of AC-side phase current. Their peaks are  
340 respectively 30.7kV and 0.28kA. With (15), the corresponding converter rating can be calculated as  
341 25.8MVA, which is slightly higher than its output reactive power.

342 As Figure 5c and 5d shown, in the conventional MMC-DDI that has no transformer, the arm  
343 voltage contains mainly AC component and the DC component only occupies a small part. The arm  
344 voltage peak is 31.5kV, slightly higher than AC phase voltage. The arm current contains mainly DC  
345 component and its peak is 1.6kA, far higher than the AC phase current. With (15), the corresponding  
346 converter rating can be calculated as 151MVA, about 6.5 times of the DC-side output power.

347 As Figure 5e and 5f shown, in the optimized MMC-DDI system that has a transformer, the arm  
348 voltage contains about 40% DC and 60% AC components, and the arm current is similar. The arm  
349 voltage and current peaks are respectively 7.2kV and 3.2kA, corresponding to a 39.9 MVA converter  
350 rating. Compared with the original MMC-DDI without transformer, the arm current peak increases  
351 by 100% while the arm voltage peak reduces by 78%, thus the converter rating is only 44% of its  
352 original value.

353 The converter characteristics in such simulation results are consistent with the above analysis  
354 and calculation. And the values of the converter voltage and current are also consistent with the  
355 theoretical results listed in Table 1. This proves the accuracy of the analysis and calculation on the  
356 MMC converter rating present in the paper.

## 357 6. Discussion and Further Improvements

358 Concerning the converter rating of MMC-DDI presented in this paper, the goal is to improve  
359 the economics of MMC-DDI while maintaining the same output de-icing characteristics. It turns out  
360 that, for a given DC ice-melting requirement, the converter rating of MMC-DDI varies greatly with  
361 its AC-side input voltage. Then it is proposed to insert a transformer on the AC side of the MMC  
362 converter so that the converter rating as well as its cost can be significantly reduced, and then the  
363 economics of MMC-DDI can be improved.

364 It seems that this proposed configuration scheme is contradict with traditional understanding  
365 of the MMC structure. Conventionally, in the common MMC system such as SVG, the AC side input  
366 transformers are expected to be avoided as much as possible.

367 This difference can be explained for the reason that the converter characteristic of MMC-DDI  
368 has significant differences with that of the common MMC system. In a SVG, both the arm voltage  
369 and current contain only AC component. As a result, in the case of a certain output power, the arm  
370 voltage is inversely proportional to arm current, thus the converter rating keeps basically constant  
371 under any AC-side voltage. In that case, if a transformer was configured on the AC side of MMC  
372 converter, it has little influence on the converter rating while increases a transformer. Therefore, in  
373 the common SVG, it tries to avoid a transformer. However, in the MMC-DDI, the arm voltage and  
374 arm current of converter contain both DC and AC components. As a result of the crossover between  
375 the DC components and the AC components, the converter rating of MMC-DDI varies greatly with  
376 its AC-side voltage. Due to such converter characteristics, a transformer can affect the converter  
377 rating. In this case, although the introduction of transformer will increase a transformer cost, it can  
378 cause a cost increment or reduction of the converter. As long as the reduction of the converter cost  
379 is sufficient to offset the transformer cost, the introduction of the transformer is cost-effective. In  
380 addition, because the unit cost of MMC converter is generally much higher than that of transformer,  
381 the above condition is easy to satisfy under the typical DC ice melting system parameters. Therefore,  
382 the optimized configuration scheme proposed in this paper is cost-effective in many cases.

383 It should be noted, the MMC-DDI can have two operation modes, ice-melting mode and SVG  
384 mode. This paper only considers the requirement of the ice melting mode, while does not analyze  
385 the operating characteristics of the SVG mode. In the optimization design process, the requirements

386 of SVG mode has not been take into account. This requirement can be further studied to get more  
387 comprehensive optimization result.

## 388 7. Conclusions

389 MMC-based ice-melting device has recognized as a promising de-icing solution. In this paper,  
390 the converter characteristic of MMC-DDI was quantitatively analyzed. It is revealed that, for a given  
391 DC ice-melting requirement, the converter rating varies greatly with its AC-side input voltage, and  
392 its minimum is 2.9 times of the output ice-melting power. When the grid access point voltage of the  
393 MMC-DDI is far more or far less than the required DC de-icing voltage, the conventional MMC-DDI  
394 structure will result in a much higher MMC converter rating than its output ice-melting power, thus  
395 the economy of the MMC-DDI is very poor.

396 In order to reduce the converter rating and then improve the economy of MMC-DDI, this paper  
397 proposes an optimized MMC-DDI configuration structure that a two-winding transformer should  
398 be inserted between the grid and the converter in some cases. As a result, the converter rating can be  
399 significantly reduced. A cost comparison of typical transformer and MMC converters was given in  
400 this paper. Considering the cost, the introduction of the transformer is cost-effective in many cases.  
401 Under the typical cost range of converter and transformer, we can get the following conclusions.

402 1) When the ratio of grid line voltage to the DC-side output ice-melting voltage exceeds 1.96 or  
403 falls below 0.25, the overall cost of MMC-DDI with transformer is less than that with no transformer,  
404 namely, a transformer should be inserted on the AC side of converter to improve system economy.

405 2) When the ratio of the grid line voltage to the DC-side output voltage is among 0.25-1.96, no  
406 transformer is required.

407 A design example and simulation results are given in this paper. In the case of outputting the  
408 same de-icing characteristics, the optimized converter rating is reduced from 151MVA to 68MVA,  
409 and the total cost of MMC-DDI is reduced by 48%. It fully proved the effectiveness of the proposed  
410 optimization design.

411 This analysis and conclusion are conducive to the optimized configuration of the modular  
412 multilevel DC de-icer, then to its engineering application for high voltage transmission lines.

## 413 Appendix A

414 **Table A1.** The minimum de-icing current and maximum endure current for typical power lines[5]

conductor type	Min. de-icing current( A ) (-5 °C, 5 m/s, 10 mm, 1 hour)	Max. endure current( A ) (5 °C, 0.5 m/s, No icing)
LGJ-4×400/50	3475	4764
LGJ-2×500/45	1989	2698
LGJ-2×240/40	1218	1716
LGJ-1×240/40	609	858
LGJ-1×185/45	515	733
LGJ-1×150/35	441	633
LGJ-1×95/55	345	500
LGJ-4×400/50	3475	4764

415 **Table A2.** Deal prices of several typical SVG projects in China from 2013 to 2018

No.	Project location	Rated Voltage ( kV )	Rating ( MVA )	Deal price <sup>1</sup> (1000 \$)	Unit cost (1000 \$/MVA)
1	Kunming, Yunnan	35	10	154	15.4
2	Zhangjiakou, Hebei	35	12	175	14.6

3	Huimin, Shandong	35	15	215	14.4
4	Huangpi, Hubei	35	16	251	15.7
5	Tongyu, Gansu	35	20	269	13.5
6	Hua County, Henan	35	20	257	12.8
7	Chenzhou, Hunan	10	20	330	16.5
8	Qiaojia, Yunnan	35	30	385	12.8
9	Linwu, Ningxia	35	40	458	11.5
10	Dabancheng, Xinjiang	35	50	615	12.3
11	Yinan, Shandong	35	60	1023	17.1
12	Haixi, Xinjiang	35	60	1154	19.2
13	Hami, Xinjiang	35	80	1508	18.8
14	Huaping, Yunnan	35	100	2109	21.1
15	Xiangtan, Hunan	35	120	2615	21.8

416 <sup>1</sup> The deal price covers a complete set of SVG equipment (including the converter chain, connection reactance,  
417 startup circuit, cooling system, control system and other ancillary facilities) and its technical service.

418 **Table A2.** Deal prices of several 10MVA-class rectifier transformers in China

No.	Project location	Rated Voltage (kV)	Rating (MVA)	Deal price (1000 \$)	Unit cost (1000 \$/MVA)
1	Baoding, Hebei	10/5	10	86	8.6
2	Changsha, Hunan	10/7	14	110	7.8
3	Changsha, Hunan	35/6	24	166	6.9
4	Xinyu, JiangXi	35/12	56	246	4.4
5	Chongqing	35/15	86	284	3.3
6	Zhuzhou, Gansu	35/17	100	323	3.2
7	Hengyang, Hunan	35/19	120	361	3.0

419

420 Author Contributions: Conceptualization, J.L. and Q.H.; Formal Analysis, Q.H.; Data Curation, X.M.,  
421 and Y.Z.; Writing-Review & Editing, S.Z.; Supervision, Y.T.

422 **Funding:** This research was funded by the science and technology project of State Grid Electric Corporation  
423 grant number 5216A016000P.

424 **Conflicts of Interest:** The authors declare no conflict of interest.

## 425 References

- 426 1. Joe. CP, Phillip. L. Present State-of-the-Art of Transmission Line Icing. *IEEE Transactions on Power*  
427 *Apparatus and Systems* 1982, 8, 2443-2450.
- 428 2. M. Farzaneh, K. Savadjiev, Statistical analysis of field data for precipitation icing accretion on overhead  
429 power lines, *IEEE Trans. Power Deliver*, 2005, 2, 1080-1087.
- 430 3. Volat C, Farzaneh M, Leblond A. De-icing/Anti-icing Techniques for Power Lines: Current Methods and  
431 Future Direction. *Proceedings of the 11th International Workshop on Atmospheric Icing of Structures*,  
432 Montreal, Canada, 2005.
- 433 4. E. B, J. A, L. S. Modelling of Ice Storms and their Impact Applied to a Part of the Swedish Transmission  
434 Network. *2007 IEEE Lausanne Power Tech 2007*, 1593-1598.
- 435 5. J. Wang, C. Fu, Y. Chen, etc., Research and application of DC de-icing technology in China southern power  
436 grid, *IEEE Trans. Power Deliver* 2012, 3, 1234-1242.

- 437 6. Joe C. Pohlman, Phillip Landers, Present state-of-the-art of transmission line icing, IEEE Trans. Power  
438 Apparatus and Systems, 1982, 1, 2443-2450.
- 439 7. Motlis Y. Melting ice on overhead-line conductors by electrical current. CIGRE SC22/WG12. Paris; 2002
- 440 8. Farzaneh M, Jakl F, Arabani MP, etc. Systems for prediction and monitoring of ice shedding, anti-icing  
441 and de-icing for power line conductors and ground wires. CIGRE, 2010.
- 442 9. Rao Hong, Licheng Li, Xiaolin Li, Chuang Fu. Study of DC based De-icing Technology in China Southern  
443 Power Grid. Southern Power System Technology 2008,2(2),7-12.
- 444 10. C. C. Davidson, C. Horwill, M. Granger, etc., Thaw point, 2007, 21(6), 26-31.
- 445 11. S. Bhattacharya, Z. Xi, B. Fardenesh, etc. Control reconfiguration of VSC based STATCOM for de-icer  
446 application, in Proc. IEEE Power Eng. Soc. Gen. Meeting, 2008, 1-7.
- 447 12. M.R. F, Ramirez D, Rey-Boue A, etc. Modular Multilevel Converters: Control and Applications. Energies  
448 2017,11,1709.
- 449 13. M. A. Perez, S. Bernet, J. Rodriguez, S. Kouro, and R. Lizana. Circuit topologies, modeling, control  
450 schemes, and applications of modular mul-tilevel converters. IEEE Trans Power Electron 2015, 1, 4-14.
- 451 14. H. Mei and J. Liu. A Novel DC Ice-melting Equipment Based on Modular Multilevel Cascade Converter.  
452 Automation of Electric Power Systems 2013, 16, 96-102.
- 453 15. Ning Y, Zheng J, Chen Z. Application of star-connected cascaded STATCOM in DC ice-melting system.  
454 Automation of Electric Power Systems 2015, 21, 1920-1922.
- 455 16. B. Li, S. Shi, D. Xu, Wei Wang, Control and Analysis of the Modular Multilevel DC De-Icer With  
456 STATCOM Functionality, IEEE Trans. Industrial Electronics 2016, 9, 5465-5476.
- 457 17. Y. Guo, J. Xu, C. Guo, etc. Control of full-bridge modular multilevel converter for dc ice-melting  
458 application, in Proc. 11th IET Int. Conf. AC DC Power Transmission 2015, 1-8.
- 459 18. IEEE Standard for Calculating the Current-Temperature Relationship of Bare Overhead Conductors. IEEE  
460 Std 738-2012, 2013, 1-72.
- 461 19. CIGRE. Thermal Behavior of Overhead Conductors .Electra, 1992, 144, 107-125.